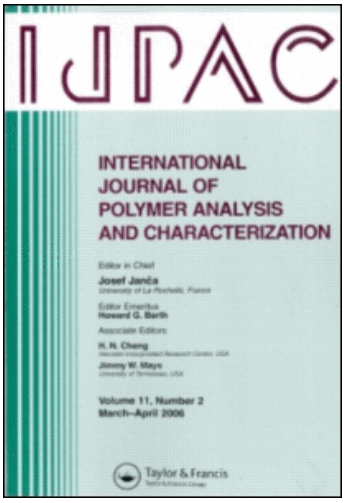

International Journal of Polymer Analysis and Characterization
Publication details, including instructions for authors and subscription information:
http://www.informaworld.com/smpp/title~content=t713646643

Sample Mass Effects on Thermal Field-Flow Fractionation Retention and Universal Calibration

Wen-Jie Cao[a]; Marcus N. Myers[a]; R. Stephen Williams[a]; J. Calvin Giddings[a]
[a] Department of Chemistry, University of Utah, Salt Lake City, UT, USA

To cite this Article Cao, Wen-Jie , Myers, Marcus N. , Williams, R. Stephen and Giddings, J. Calvin(1998) 'Sample Mass Effects on Thermal Field-Flow Fractionation Retention and Universal Calibration', International Journal of Polymer Analysis and Characterization, 4: 5, 407 — 433
To link to this Article: DOI: 10.1080/10236669808009726
URL: http://dx.doi.org/10.1080/10236669808009726

Int. J. Polym. Anal. Charact.,
1998 Vol. 4, pp. 407–433
Reprints available directly from the publisher
Photocopying permitted by license only

Sample Mass Effects on Thermal Field-Flow Fractionation Retention and Universal Calibration*

WEN-JIE CAO, MARCUS N. MYERS†, P. STEPHEN WILLIAMS and J. CALVIN GIDDINGS‡

Department of Chemistry, University of Utah, Salt Lake City, UT 84112, USA

(Received 8 October 1997; In final form 3 April 1998)

The effect of sample mass on retention in thermal field-flow fractionation (FFF) can be large, becoming more important as the molecular weight increases. Greater retention with increased sample mass is observed beginning at the detection limit of 0.1 μg of polystyrene in tetrahydrofuran (THF) with higher molecular weight material. Empirical equations have been developed to correct for changes in calibration parameters for the thermal FFF universal calibration curves due to the sample mass effect on polymer retention for polystyrene, polymethylmethacrylate, and polyisoprene in THF.

Keywords: Thermal FFF; Sample mass; Retention; Universal calibration

INTRODUCTION

Thermal field-flow fractionation (ThFFF) is a proven technique for polymer separation and characterization.[1] The poor understanding of thermal diffusion in ThFFF requires using polymer standards for obtaining a calibration curve to establish the relationship between

* Presented at the 10th International Symposium on Polymer Analysis and Characterization (ISPAC-10), Toronto, Canada, August 11–13, 1997.

† Corresponding author.

‡ Deceased October 24, 1996.

polymer retention and molecular weight. Giddings[2] proposed that the calibration for ThFFF is universal enabling the transfer of calibration parameters obtained on one ThFFF instrument to other units for a given polymer–solvent pair because the calibration parameters are determined by the physicochemical constants D and D_T, the common diffusion and the thermal diffusion coefficients, respectively. This is in contrast to the universal calibration used in SEC which requires the calibration of each individual column, but, in theory, applies to all polymers which behave similarly to the polymer used for calibration.

Varying sample mass is thought to give rise to some of the observed variation in the calibration curves found in our laboratory and in those of other investigators.[3–5] Variation of sample retention with sample mass has been called overloading, usually accompanied by skew, increased width, or other peak shape changes, or even multiple peak formation. Caldwell *et al.*[6] examined this overloading effect in an effort to determine upper limits to sample concentration below which retention time would be independent of sample concentration. Recent work using more sensitive detectors has indicated the sample mass effects of band broadening, skewed peaks and longer retention continue to much smaller sample masses and modify the calibration curves. The amount of sample injected can affect the retention time primarily by influencing the viscosity of the solute–solvent mixture in the sample zone. The increased viscosity decreases the zone velocity, resulting in longer retention. In ThFFF, the concentration across the channel thickness varies due to the migration of the molecules under the influence of the temperature gradient. The concentration distribution is approximately exponential as given by

$$c(x) = c_0 \exp(-x/\lambda w), \tag{1}$$

where $c(x)$ is the concentration at distance x across the channel thickness measured from the so-called accumulation wall, c_0 is the concentration at the accumulation wall, w is the channel thickness, and λ the retention parameter or reduced mean thickness of the sample zone. Shortly after injection, the sample zone is assumed to broaden into a Gaussian distribution along the z-axis corresponding to the direction of flow down the channel. The two dimensional concentration

becomes[7]

$$c(x,z) = c_{00} \exp\left[\frac{-(z-Z)^2}{2\sigma^2}\right] \exp\left[\frac{-x}{\lambda w}\right], \tag{2}$$

where Z is the distance traveled by the center of the zone down the channel. The concentration at the accumulation wall at the center of the zone, c_{00}, is found from[6]

$$c_{00} \cong \frac{V_{\text{inj}} c_{\text{inj}} L}{(2\pi\sigma^2)^{1/2} V^0 \lambda}, \tag{3}$$

where V_{inj} is the volume of sample injected, V^0 is the void volume, c_{inj} is the concentration of the injected sample, L is the length of the channel, and σ^2 is the sum of the variances contributing to the zone breadth, given by

$$\sigma^2 = \sigma_{\text{inj}}^2 + \sigma_{\text{neq}}^2 + \sigma_{\text{poly}}^2, \tag{4}$$

where

$$\sigma_{\text{inj}}^2 = \frac{1}{12}\left[\frac{V_{\text{inj}} L}{V^0}\right]^2 \tag{5}$$

and

$$\sigma_{\text{neq}}^2 = \chi(\lambda) w^2 \langle v \rangle \frac{Z}{D} \tag{6}$$

in which $\langle v \rangle$ is the mean carrier velocity of the carrier. The nonequilibrium coefficient $\chi(\lambda)$ is given at high retention by

$$\chi(\lambda) = 24\lambda^3. \tag{7}$$

The variance due to the polydispersity of the polymer is described by

$$\sigma_{\text{poly}}^2 = Z^2 \left(\frac{\mathrm{d} \ln V_{\text{r}}}{\mathrm{d} \ln M}\right)^2 (\mu - 1), \tag{8}$$

where μ is the ratio of the weight to number average molecular weights and $(\mathrm{d}\ln V_r/\mathrm{d}\ln M)$ is the selectivity corresponding to the relative change in elution volume V_r divided by the relative change in molecular weight M.

Data for the effect of concentration on the viscosity are rarely reported since most workers are interested in the intrinsic viscosity $[\eta]$ which can be related to the molecular weight by the Mark–Houwink relationship

$$[\eta] = KM^a, \tag{9}$$

where K and a are determined from the extrapolation of viscosity–concentration measurements to zero concentration. For low concentrations, the viscosity can be estimated using the Huggins relationship[8]

$$\left(\frac{\eta - \eta_0}{\eta_0 c}\right) = [\eta](1 + k_H[\eta]c) \tag{10}$$

with η_0 being the viscosity of the pure solvent and k_H, the Huggins coefficient. The effect of temperature on the viscosity of the carrier can be expressed as

$$\frac{1}{\eta} = a_0 + a_1 T + a_2 T^2 + a_3 T^3, \tag{11}$$

where a_0, a_1, a_2, and a_3 are empirically obtained coefficients.

The velocity of the flow stream across the channel can be described by [9]

$$v(x) = -\frac{\mathrm{d}p}{\mathrm{d}z}\left[\int_0^x \frac{x}{\eta(x)}\,\mathrm{d}x - \frac{\left(\int_0^w (x/\eta(x))\,\mathrm{d}x\right)}{\left(\int_0^w (1/\eta(x))\,\mathrm{d}x\right)}\left(\int_0^x \frac{1}{\eta(x)}\,\mathrm{d}x\right)\right], \tag{12}$$

where $v(x)$ is the laminar flow velocity at position x, x is the coordinate across the channel thickness w, $\mathrm{d}p/\mathrm{d}z$ is the pressure gradient along the channel length L, and $\eta(x)$ is the local fluid viscosity.

In the region of the zone, η varies with x because of the gradient in both temperature and concentration. The effects act together to

increase the viscosity towards the cold wall. Only the temperature gradient influences viscosity and the velocity profile in front of and behind the zone. Within the zone the velocity profile is more distorted than in the rest of the channel. This is illustrated in Figure 1(a) and (b) where flow velocity profiles at the center of the zone are compared with the isothermal and the temperature corrected pure solvent velocity profiles. The curves are calculated for a 20 μg sample of polystyrene (PS) in toluene. The viscosity data for 250 kg/mol were obtained from Streeter and Boyer,[10] and the 1000 kg/mol viscosity estimated using Equation (10). The effect of molecular weight is readily apparent, with much lower velocities close to the cold wall for the higher molecular weight material.

The mean flow velocity must remain constant along the channel length (due to conservation of mass). To bring about the change in velocity profile there must be an x-component to the flow as the concentration profile changes along the length of the zone. There is a

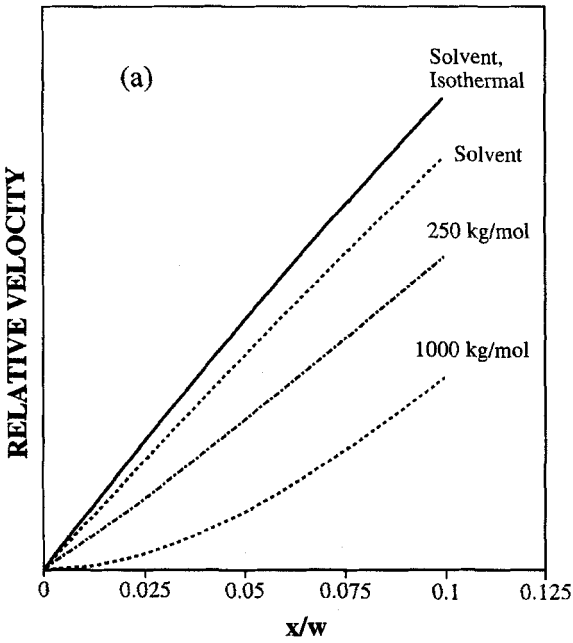

FIGURE 1(a)

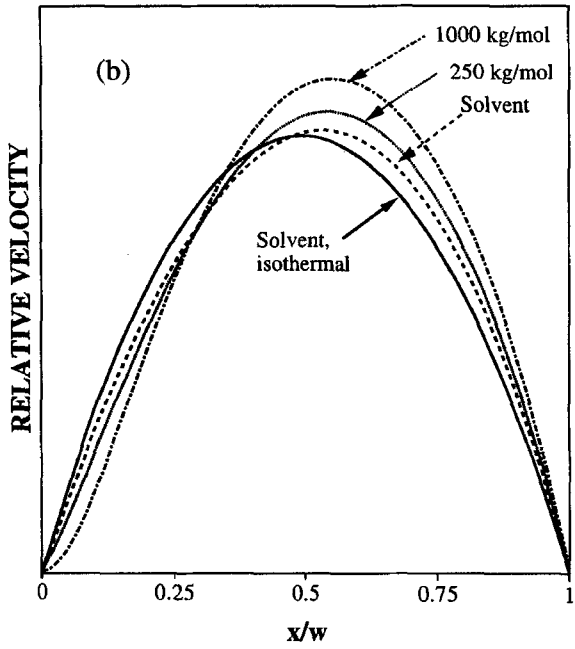

FIGURE 1(b)

FIGURE 1 Relative velocity profile in a ThFFF channel illustrating the effect of the presence of polymer on the velocity profile. Calculations are for a 20 μg sample of PS in toluene following migration of 2 cm from injection with $\Delta T = 50°C$ and $T_c = 25°C$, (a) details of profiles close to the cold wall, (b) the profiles across the entire channel.

tendency for the carrier fluid to flow over the top of the zone, with increased velocity in the region above the body of the zone. This is only a partial diversion of flow, as the zone keeps moving at a slower velocity than if there were no additional distortion of velocity profile, as shown in Figure 1(b).

The viscosity corrections used here are simplified to illustrate the effects of concentration of the polymer on the flow profile. The actual viscosity–concentration dependence may be considerably more complicated. Some authors have divided the concentration effect on viscosity into three regions,[11] the dilute region $c < c^*$ (where c^* is the concentration where polymer coils overlap), the transition region $c^* < c < c^{**}$ (where c^{**} is the concentration above which pseudo-gel behavior is observed), and the semidilute region $c > c^{**}$. Callaghan

and Pinder[12] show that the gel behavior is only observed when $c/c^* > 5$ for 110 kg/mol PS in CCl_4 at 25°C. For PS in THF at 25°C, Yu *et al.*[11] obtained the following equations for c^* and c^{**}:

$$\log c^* = 2.436 - 0.725 \log M, \tag{13}$$

$$\log c^{**} = 3.416 - 0.8 \log M, \tag{14}$$

where concentration has units of g/mL.

Increased concentration, particularly due to the enhanced concentration near the cumulative wall induced by the thermal field, may allow the polymer coils to entangle to the extent that a gel or pseudo-gel may be formed. For large polymers like 1000 kg/mol PS, the concentration enhancement could be many times the original injected concentration. Gelation of PS in a large number of solvents was attempted by Tan *et al.*[13] Only 14 liquids, most of them relatively poor solvents, were found capable of gel formation. In THF, PS gel formed at temperatures from −100°C to −70°C and at concentrations from 150 to 300 mg/mL, respectively. The gelation temperature range was much lower than the cold wall temperature T_c (25°C) and the concentration was much higher than c_{00} in our experiments. It appears that permanent gel formation would not occur in the present study.

The behavior of a pseudo-gel solution is quite different from the polymer solution from which it is formed. The diffusion coefficient of a pseudo-gel is much smaller than that of the original polymer, while the viscosity of the pseudo-gel solution will be much larger than the original polymer solution. The pseudo-gel, in theory, will be compressed closer to the cold wall and elute out of the channel later than the parent molecule. However, as the size of the pseudo-gel cluster increases, hydrodynamic effects will result in an earlier emergence from the channel. If either of these scenarios occur in the ThFFF channel, double peaks might be observed with a given molecular weight sample.

An additional complication occurs as the concentration decreases in the zone as it moves down the channel. The quantitative description of the viscosity effect in the region of the zone is very complicated and beyond the scope of this paper. However, the qualitative effects on the velocity profile as illustrated explain the change in retention observed even at small concentrations.

Since, from theory,[1]

$$\lambda\Delta T = \frac{D}{D_T}, \tag{15}$$

any effect of concentration on diffusion becomes important. Below c^*, the diffusion coefficient can be described by the expression[8]

$$D = D_0(1 + k_D c), \tag{16}$$

where D_0 is the diffusion coefficient at zero concentration. For polystyrene in THF, k_D is positive and the diffusion rate increases with increased concentration. From Equation (15), such an increase in D would lead to less retention or a larger $\lambda\Delta T$ with a corresponding change in the calibration curve as shown by Figure 2 which considers

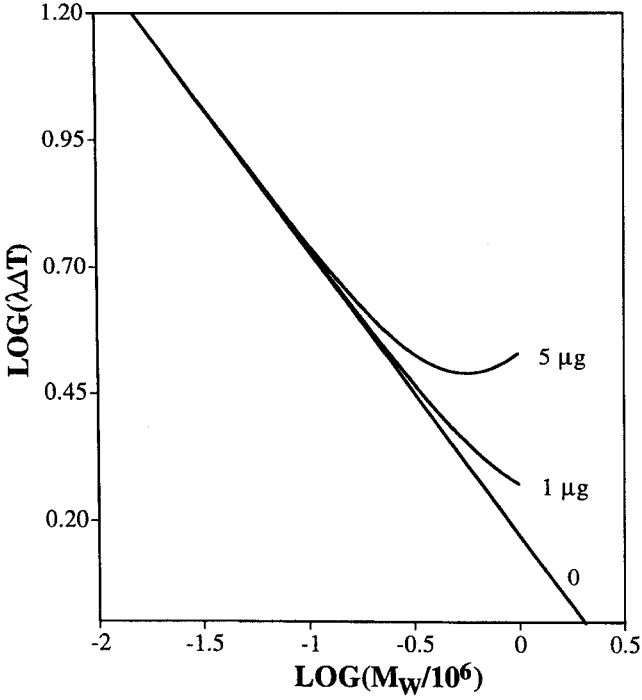

FIGURE 2 Effect of concentration on the calibration curve of PS in THF if only diffusion is affected.

only the concentration effect on D, assuming D_T remains constant with concentration.

Concentration effects on D_T are not clearly understood, since conflicting results are reported in the few existing studies. For PS, Hoffman and Zimm[14] and Whitmore[15] found no dependence in a poor solvent, while using a good solvent resulted in a small change with concentration.

If the carrier viscosity, the thermal conductivity, and the thermal diffusion ratio are considered constant in the temperature gradient, the retention volume can be translated into the dimensionless retention parameter λ by the general equation[1] for FFF,

$$R = \frac{V^0}{V_r} = 6\lambda\left(\coth\frac{1}{2\lambda} - 2\lambda\right), \tag{17}$$

where V^0 is the void (channel) volume, and V_r is the sample retention volume. The use of a thermal field requires adjustment for the effect of temperature on viscosity η and the change in thermal conductivity across the channel, resulting in a more complex equation for defining λ from retention data, utilizing Equation (12).

The common diffusion coefficient can be related to polymer molecular weight by the well-known equation,

$$D = A(M_w)^{-b}, \tag{18}$$

where M_w is the polymer molecular weight, A and b are constants reflecting the polymer chain stiffness in a solvent and the interaction strength between the polymer chains and the solvent, etc.

Dividing Equation (18) by D_T, and substituting into Equation (15), we obtain

$$\lambda\Delta T = \frac{D}{D_T} = \frac{A}{D_T}(M_w)^{-b}. \tag{19}$$

Schimpf and Giddings[16,17] showed that D_T is independent of polymer molecular weight although Myerhoff and Rauch,[18] Hoffman and Zimm,[14] and Whitemore[15] showed that D_T is slightly dependent on molecular weight for some polymer–solvent combinations. Assuming that the following relationship between D_T and molecular

weight exists,

$$D_T = B(M_w)^{\beta}, \tag{20}$$

where B and β are two constants, we may substitute Equation (20) into Equation (19) to obtain

$$\lambda \Delta T = \phi (M_w)^{-n}, \tag{21}$$

where

$$\phi = A/B, \tag{22}$$

and

$$n = b + \beta. \tag{23}$$

In order to avoid extrapolating to unit polymer molecular weight to obtain the value of ϕ, Giddings[2] recommended a similar equation,

$$\lambda \Delta T = \phi_6 \left(\frac{M_w}{10^6} \right)^{-n}, \tag{24}$$

where

$$\phi_6 = \phi (10)^{-6n}. \tag{25}$$

Here, ϕ_6 and n are the ThFFF universal calibration parameters which can be obtained from the intercept and the slope of the plot of $\log(\lambda \Delta T)$ versus $\log(M_w/10^6)$. Since there are no ThFFF system parameters such as channel thickness, length, and breadth in Equation (24), and no packing material inside the channels, the ThFFF calibration parameters n and ϕ_6 are expected to be system (channel) transferable. Once ϕ_6 and n are measured for a polymer–solvent pair, they may be used with any ThFFF channel.

In previous papers,[19,20] the effect of cold wall temperature on polymer ThFFF retention and universal calibration has been addressed extensively. Those results showed that although polymer ThFFF retention could be manipulated by changing the cold wall

temperature, the value of n remains constant for a given polymer–solvent pair. Only ϕ_6 was shown to be dependent on the cold wall temperature.

EXPERIMENTAL

Two newer ThFFF channels,[20] which have a uniform temperature profile along the channel length, were used in this experiment. Both ΔT and T_c could be controlled to within $\pm 1°C$. Dimensions of the two spacers used are listed in Table I. The data for PS were collected on channel 20. The data for polymethylmethacrylate (PMMA) and polyisoprene (PIP) were collected on channel 21.

SSI II (FFFractionation, L.L.C., Salt Lake City, UT) pumps were used to deliver carrier (THF). A Varex (model ELSD IIA) evaporative light-scattering detector (Varex Corporation, Burtonsville, MD) was used to detect polymer peaks of PMMA and PIP. A Spectroflow 757 (Applied Biosystems, Ramsey, NJ) UV HPLC detector was used for PS detection at a wavelength of 254 nm.

The dead volume of the ThFFF system was subtracted from retention volumes for accurate calculation.

The detector signal was recorded by an Omniscribe® Recorder chart recorder (Houston Instrument, Austin, TX) for the original fractogram and by an IBM compatible PC (AT 286) for data collection. In-house software was used for all data collection and processing.

Polymer standards were obtained from Polymer Standards Service (Polymer Standards Service-USA, Silver Spring, MD). Their parameters are listed in Table II.

Fisher Chemical HPLC grade THF (Fisher Scientific, Fair Lawn, NJ) was used as carrier and solvent for the polymer standards.

TABLE I The dimensions of the spacers used in the ThFFF channels

Channels	*Materials*	$L_{tip-tip}$ (cm)*	*Breadth* (cm)	*Thickness* (cm)	V^0 (cm^3)†
20	Polyimide‡	27.5	2	0.0127	0.622
21	Polyimide‡	33.2	1.6	0.0127	0.620

* Tapered at both ends.
† Geometric volume.
‡ Teflon coated.

TABLE II Molecular weights and polydispersities of polymer standards

Polymers	M_p (kg/mol)	M_w (kg/mol)	M_n (kg/mol)	M_w/M_n
PS	34.3	33.5	32.6	1.03
	99.4	96	92.4	1.03
	273	257	245	1.05
	556	546	536	1.02
	1000	944	880	1.07
PMMA	37	37	35	1.04
	100	97	91	1.04
	280	270	255	1.05
	570	570	550	1.03
PIP	140	108	104	1.04
	293	293	287	1.02
	1050	963	860	1.12

The stock sample solution was made at least 24 h before the experiments to ensure solvation. In these experiments, a very small amount (≈ 0.0001 mg/mL) of the antioxidant Irganox® 1010, (Ciba-Geigy Corporation, Hawthorne, NY) was added to the stock solution to prevent THF peroxide formation and polymer degradation, and also to supply a signal for void peak detection.

A Rheodyne (Cotati, CA) model 7125 syringe loading sample injector was used for sample injection. The volume of the sample loop was 20 μL.

The cold wall temperature was controlled to 25 ± 1°C and the carrier flow rate was 0.1 mL/min for all experiments. The ΔT was controlled to 50 ± 1°C for PS and PMMA, and 70 ± 1°C for PIP if not otherwise indicated in the text.

RESULTS AND DISCUSSION

The results of Caldwell *et al.*[6] show that FFF overloading varied for a given sample mass ($m = V_{inj} * c_{inj}$) when larger sample volumes were used. However, the sample volumes were often quite large compared with the channel void volume (up to 13% of V^0) which would result in a broad sample zone with a loss in resolution. Such broad zones complicate the determination of the concentration in the zone. Injection concentrations ranged from 1 to 25 mg/mL and sample masses varied from 10 to 4000 μg. Both volumes and concentrations were much higher than those used in this research, where injection concentrations

were from 0.0049 to 1 mg/mL and sample masses were from 0.1 to 20 μg (only a few were 50 and 100 μg to show the extremes). Significant injection volume effects on polymer retention and the ThFFF universal calibration parameters at such low injection concentrations and sample masses were not expected. However the use of the same sample volume should give sample zones with the same starting width and the mass effect can be better seen, especially if aggregates form under the operating conditions. A sample volume of 20 μL was used for all samples.

The detector limits for this study were 0.09 μg of sample mass for 1000 kg/mol PS using a UV detector, and 1 μg for 570 kg/mol PMMA and 2.5 μg for 1050 kg/mol PIP with the ELSD. The retention was measured for sample masses ranging from these limits to more than 20 μg and was consistently found to increase with increases in sample mass. The ThFFF fractograms of Figures 3–5 illustrate both the

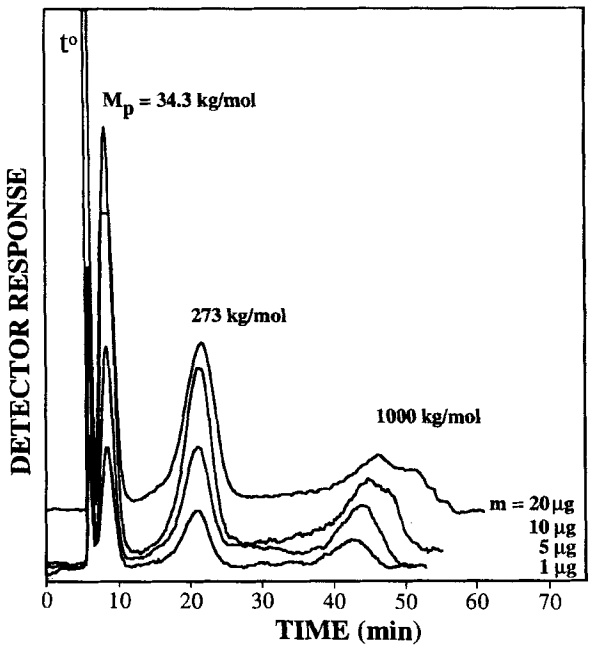

FIGURE 3 Fractograms of PS in THF showing the effect of sample mass on retention. Double-topped peak of the 1000 kg/mol PS was observed as sample mass was increased to 20 μg. $\Delta T = 50°C$. $T_c = 25°C$ and the carrier flow rate = 0.1 mL/min for all experiments.

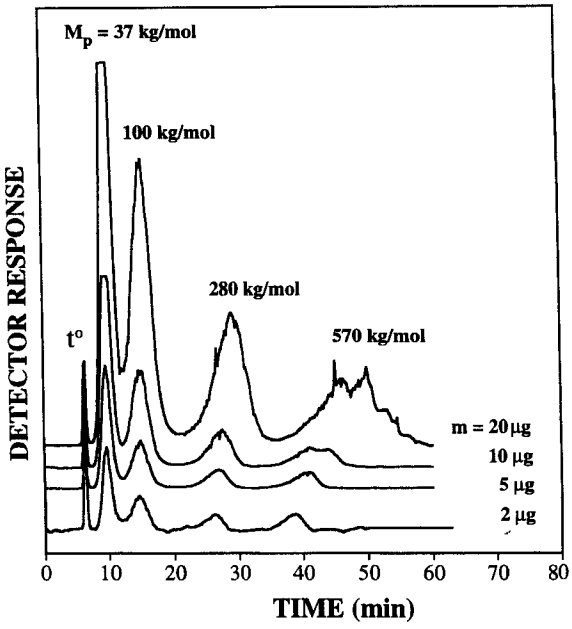

FIGURE 4 Fractograms of PMMA in THF showing the effect of sample mass on retention. Double-topped peak of the 570 kg/mol PMMA was observed as sample mass increased to 20 μg. $\Delta T = 50°C$.

increased retention and the change in peak shape as the sample mass is increased, with the greatest effects occurring for the higher polymer molecular weights. In the low sample mass range (< 10 μg), the peak shape is close to Gaussian. When the sample mass is increased to about 20 μg, second peaks appeared following the 1000 kg/mol PS and the 570 kg/mol PMMA peaks resulting in doublets as shown in Figures 3 and 4. The PS fractograms in Figure 3 were obtained at $\Delta T = 50°C$, while those in Figure 6 were collected at $\Delta T = 25°C$ showing a reduction in the effect with decrease of field strength (ΔT). This is because the concentration of polymer in the zone does not reach such high levels with the reduced ΔT.

Much of the work done in the past has been with sample amounts above 10 μg due to the relatively poor sensitivity of the detectors available at that time.[3,5,21] Larger sample masses tended to be used for higher molecular weight polymers to offset the dilution of the peaks

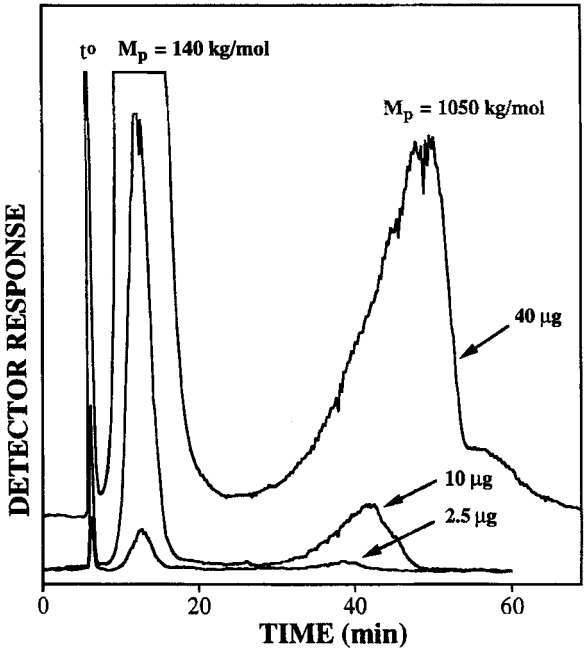

FIGURE 5 Fractograms of PIP in THF showing the effect of sample mass on retention. $\Delta T = 70°C$.

during their longer retention which results in broader and less easily detected peaks.[22] The sample concentration range used by Caldwell *et al.*[6] ranged from 1 to 25 mg/mL and the sample mass ranged from 10 to 4000 µg. They observed behavior similar to that shown in Figure 3 for sample masses above 10 µg, and suggested that this nonideal behavior might be attributable to the fact that zone concentration reaches the levels greater than c^* close to the cold wall.

As indicated above, the doublet peaks may be the result of pseudogel formed in the region of enhanced concentration near the cold wall. Equation (3) can be used to calculate the highest concentration in the zone, c_{00}, of the "relaxed" sample zone at the cumulative wall.[6] The calculated c_{00} for different c_{inj} and sample mass are listed in Table III for 1000 kg/mol PS and 37 kg/mol PMMA at $\Delta T = 50°C$ after migrating 2 cm down the channel from injection. Table III shows that the injection concentration could be enhanced as much as 45 times for

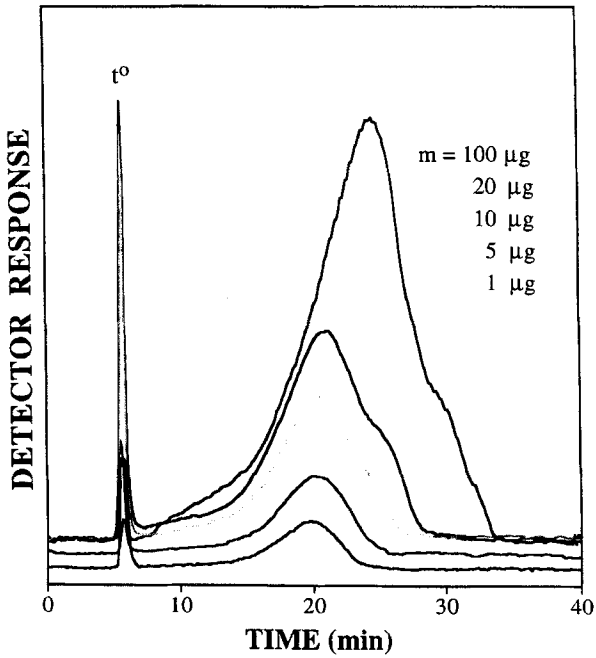

FIGURE 6 Sample mass effect for 1000 kg/mol PS at $\Delta T = 25°C$.

TABLE III Sample masses (m) injected into the channel, concentration of sample solution, calculated maximum concentration in the zone of 2 cm from injection, and the ratio of c_{00}/c_{inj} for the 1000 kg/mol PS and the 37 kg/mol PMMA at $\Delta T = 50°C$

m (μg)	c_{inj} (mg/mL)	c_{00} (mg/mL)		c_{00}/c_{inj}		c_{00}/c^*	
		PS (1000 kg/mol)	PMMA (37 kg/mol)	PS (1000 kg/mol)	PMMA (37 kg/mol)	PS (1000 kg/mol)	PMMA (37 kg/mol)
50	2.5	114.7		45.9		20.3	
20	1	41.4	5.8	41.4	5.8	7.3	0.09
10	0.5	19.4	2.9	38.7	5.7	3.4	0.04
6.2	0.31	11.6		37.3		2.0	
5	0.25	9.2	1.4	36.9	5.7	1.6	0.02
3.1	0.16	5.6		36.2		0.99	
2	0.1	3.6	0.57	35.6	5.7	0.63	0.009
1	0.05	1.7	0.28	34.9	5.6	0.31	0.004
0.56	0.028	0.97		34.4		0.17	
0.3	0.015	0.50		33.7		0.088	
0.1	0.0049	0.16		33.5		0.029	

large polymers like 1000 kg/mol PS and 5.8 times for small polymers like 37 kg/mol PMMA. Literature values of c^* for PS + THF vary, thus, Equation (13) was chosen to calculate the values of c^* in Table IV. Equation (14) was used to calculate c^{**} values for PS in THF which are also listed in Table IV. When the assumed sample amounts injected reach 20 μg for 1000 kg/mol PS, $c_{00}/c^* > 5$ and $c_{00} > c^{**}$, and conditions are such that pseudo-gel might be expected to form. Doublet peaks for 1000 k PS were observed in our experiments at 20 μg (Figure 3). As reported by Caldwell *et al.*,[6] doublet peaks (or second peaks) were observed for 860 kg/mol PS for sample masses larger than about 20 μg. Pseudo-gels would be expected to form in many of their experiments if the results of Callaghan and Pinder[12] are correct.

As stated above, retention was still found to be dependent on the sample mass at the detection limit of the detector as shown in Figure 7 for 1000 kg/mol PS and 1050 kg/mol PIP in THF. Overloading could not be eliminated, but was reduced by lowering the field strength (ΔT) from 50°C to 25°C as shown in Figure 8. Peak distortion was still apparent at larger sample masses for the 1000 kg/mol polymer at the lower ΔT as shown in Figure 6.

It appears the sample mass effect exists for all the polymers, although to a lesser extent for smaller polymers. In order to show the sample mass effect for all the polymers of a polymer family in one plot, we first obtained the values of R^0, the retention ratio for infinitely dilute concentration, by extrapolating the R versus sample mass m plot to zero sample mass, using a second-degree polynomial fit. The values of R^0 given in Table V are not exact because of the difficulty of extrapolation using this type of fitting equation, however the trend

TABLE IV Some important constants and parameters for PS in THF used in this study

M_p (kg/mol)	34.3	99.4	257	556	1000
$D_0 \times 10^{-7}$ (cm^2/s)*	9.66	5.33	3.06	2.00	1.47
k_D (mL/g)*	0.011	0.026	0.058	0.105	0.162
c^* (mg/mL)†	140	65	31	19	12
c^{**} (mg/mL)‡	613	262	117	66	41

* Calculated from the data in Ref. [23].
† Calculated from Equation (13).
‡ Calculated from Equation (14).

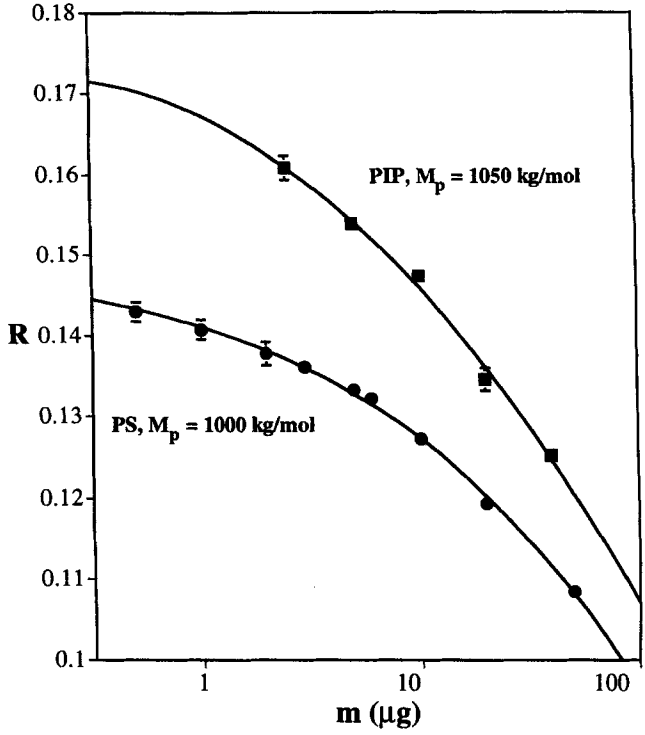

FIGURE 7 The sample mass effects on the retention ratio of 1000 kg/mol PS and 1050 kg/mol PIP in THF. Error bars correspond to one standard deviation. $\Delta T = 50°C$.

is shown. The values of R^0/R versus m are plotted in Figure 9(a)–(c) for PS, PMMA, and PIP in THF, respectively.

Figure 10 shows $\lambda\Delta T$ is dependent on both ΔT and sample mass in the sample mass range 2–20 μg. The $\lambda\Delta T$ curves for the three ΔT of 25°C, 35°C, and 50°C appear to converge to a value of about 1.5 for the 1000 kg/mol PS as sample mass approaches zero. This ΔT dependence of $\lambda\Delta T$ caused by sample mass variation may explain why different laboratories obtained different $\lambda\Delta T$ values for a given polymer under similar experimental conditions. Table VI lists some previously published $\lambda\Delta T$ values with T_c of $\sim 25°C$. The calibration parameters for the ThFFF calibration with PS in THF are also listed.

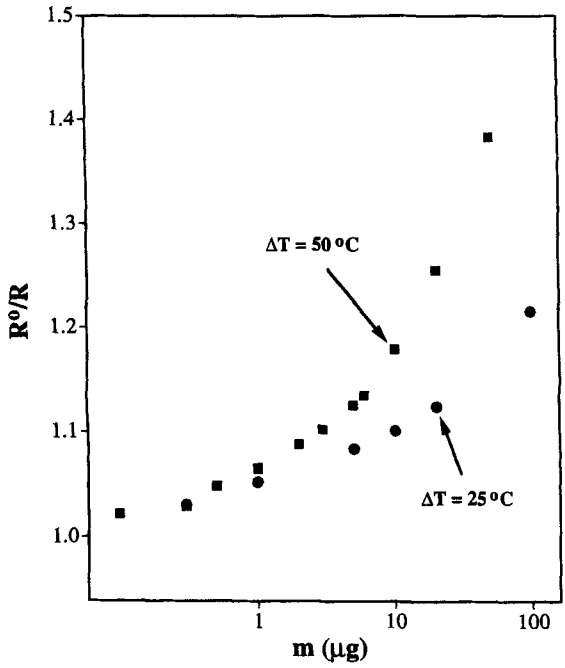

FIGURE 8 The sample mass effects on the retention ratio of 1000 kg/mol PS at $\Delta T = 50°C$ and 25°C.

TABLE V Values of R, λ, and D/D_T at infinitely dilute concentration at $T_c = 25°C$

	M_p (kg/mol)	ΔT (°C)	R^0	λ^0	$\lambda^0 \Delta T = D^0 D_T^0$ (°C)
PS					
	34.3	50	0.710	0.209	10.5
	99.4	50	0.480	0.110	5.52
	273	50	0.288	0.0628	3.14
	556	50	0.200	0.0414	2.07
	1000	50	0.147	0.0297	1.49
	1000	35	0.214	0.0426	1.49
	1000	25	0.298	0.0596	1.49
PMMA		50			
	37		0.646	0.177	8.87
	100		0.422	0.0965	4.83
	280		0.236	0.0497	2.48
	570		0.160	0.0327	1.63
PIP		70			
	140		0.490	0.122	8.51
	293		0.346	0.0792	5.54
	1050		0.165	0.0354	2.48

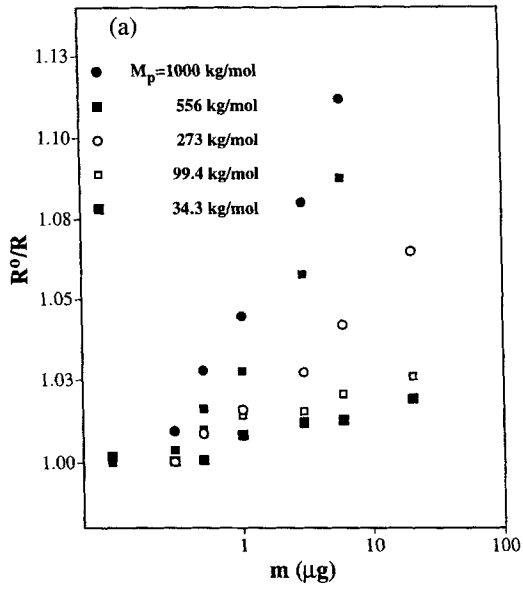

FIGURE 9(a)

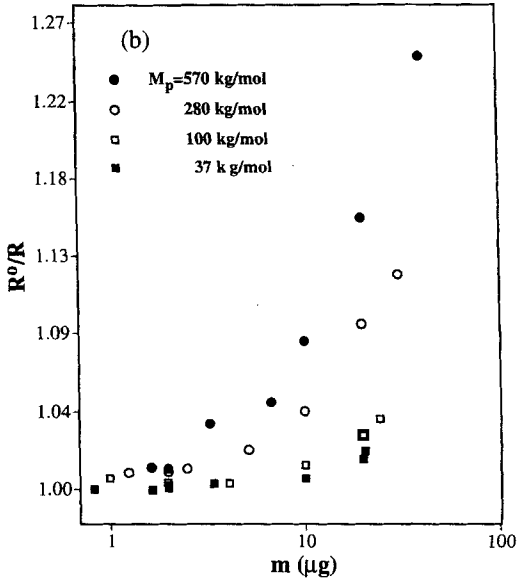

FIGURE 9(b)

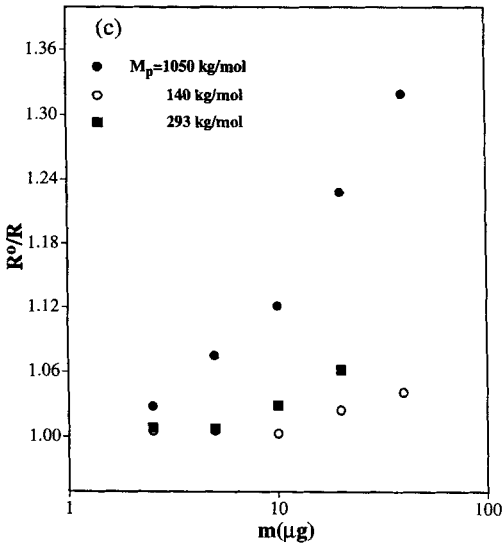

FIGURE 9(c)

FIGURE 9 The influence of sample mass on R^0/R; (a) PS in THF at $\Delta T = 50°C$, (b) PMMA in THF at $\Delta T = 50°C$, (c) PIP in THF at $\Delta T = 70°C$.

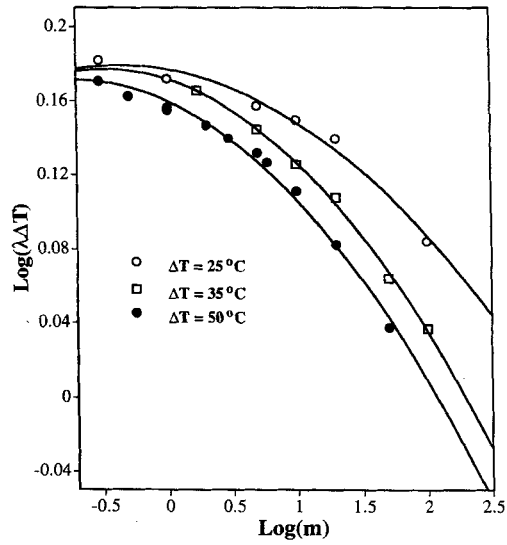

FIGURE 10 The $\lambda\Delta T$ of different ΔT (25°C, 35°C, and 50°C) versus sample mass for 1000 kg/mol PS in THF.

TABLE VI Values of $\lambda\Delta T$, n and ϕ_6 of PS in THF from different laboratories

MW (kg/mol)	T_c (K)	ΔT (K)	m (μg)	$\lambda\Delta T$ (K)	n	ϕ_6
M_p[4]	298	40	1–6		0.592	1.51
23				14.1		
35				11.0		
47.5				9.15		
90				6.27		
207.7				3.82		
400				2.59		
575				2.09		
900				1.60		
MW[5]	296	40	15–30		0.622	1.05
47.5				7.24		
110				4.12		
233				2.32		
470				2.04		
1200				0.80		
3000		30		0.57		
MW[3]						
35–900	295	40	N/A*		0.774	1.22
35				19.1		
110				5.64		
200				4.18		
470				1.98		
670				1.74		
900				1.48		

* Sample mass is not available.

Other literature values are available, but for these the sample masses are not given.[3]

When the calibration curves from different sample masses are plotted on one figure (Figure 11(a–c) for PS, PMMA, and PIP, respectively), they clearly show that the slope n increases and the intercept ϕ_6 decreases with increased sample mass.

This sample mass effect on n and ϕ_6 may explain the variation of the published values. Table VI shows that n and ϕ_6 values (0.592 and 1.51) for PS–THF pair in Ref. [4] with 1–6 μg sample mass agree with those for the 1–2 μg sample mass obtained in the present study (see Figures 12 and 13). In Ref. [5], the sample mass was larger (15–30 μg), their n value for PS–THF pair is larger (0.622) which agrees with the n value of the 15 μg sample mass in this study (see Figure 12).

The empirical equations obtained to relate n and ϕ_6 to sample mass are listed below for the three polymer–solvent pairs at $T_c = 25°C$.

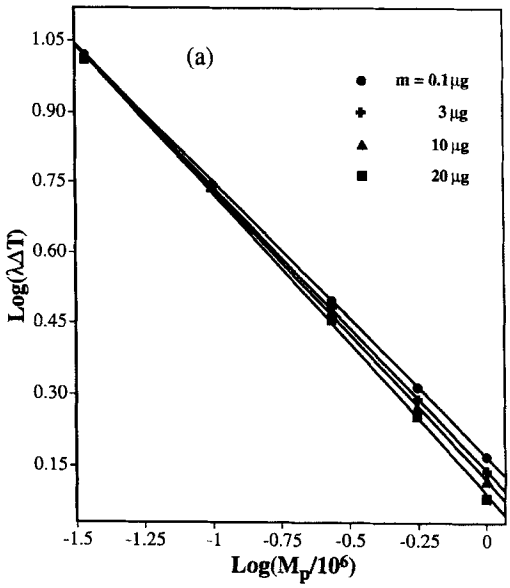

FIGURE 11(a)

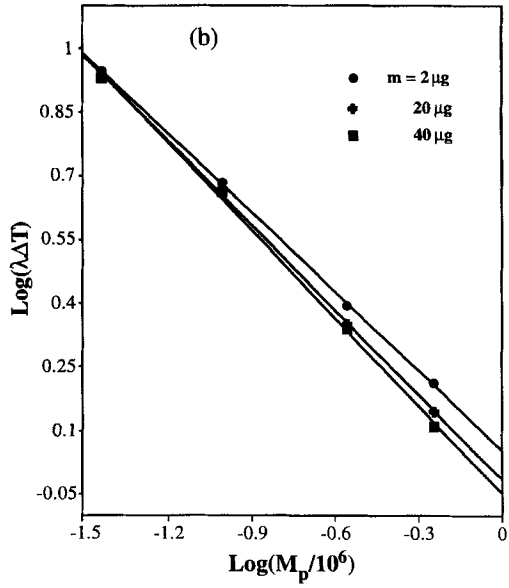

FIGURE 11(b)

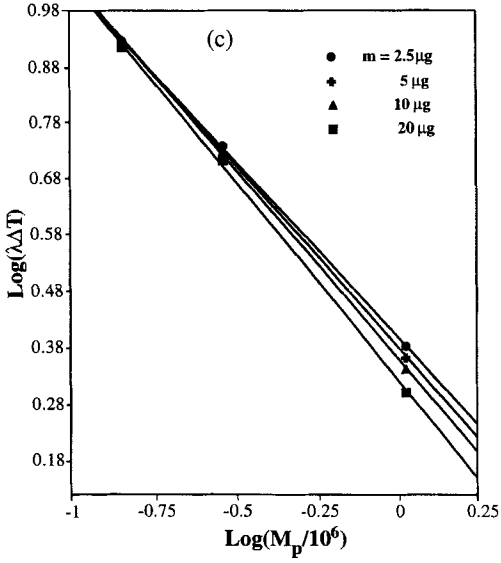

FIGURE 11(c)

FIGURE 11 The ThFFF calibration curves for different samples masses; (a) PS, (b) PMMA, (c) PIP.

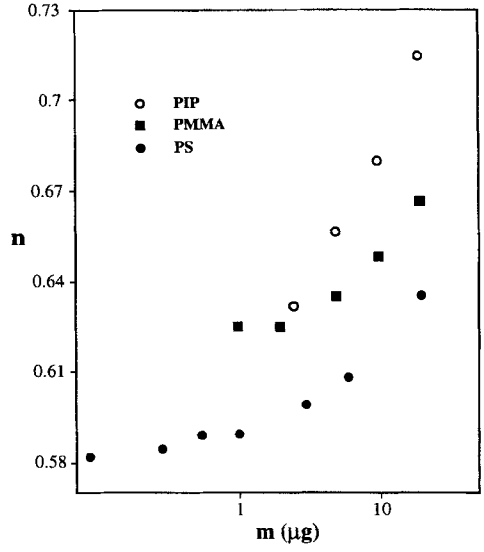

FIGURE 12 The effect of sample mass on the calibration parameter *n*.

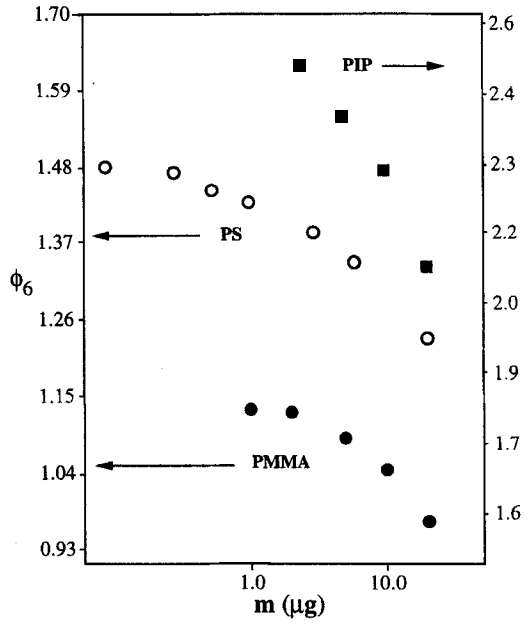

FIGURE 13 The effect of sample mass on the calibration parameter ϕ_6.

PS–THF, $\Delta T = 50°C$, for $m = 0.1–20\,\mu g$:

$$n = -1.2 \times 10^{-4} m^2 + 4.95 \times 10^{-3} m + 0.584, \quad (26)$$

$$\phi_6 = 7.9 \times 10^{-4} m^2 - 2.76 \times 10^{-2} m + 1.47. \quad (27)$$

PMMA–THF, $\Delta T = 50°C$, $m = 1–20\,\mu g$:

$$n = -4.0 \times 10^{-5} m^2 + 3.13 \times 10^{-3} m + 0.621, \quad (28)$$

$$\phi_6 = 1.3 \times 10^{-4} m^2 - 1.15 \times 10^{-2} m + 1.15. \quad (29)$$

PIP–THF, $\Delta T = 70°C$, $m = 2.5–20\,\mu g$:

$$n = -1.8 \times 10^{-4} m^2 + 8.60 \times 10^{-3} m + 0.614, \quad (30)$$

$$\phi_6 = 5.3 \times 10^{-4} m^2 - 3.44 \times 10^{-2} m + 2.57. \quad (31)$$

Application of these equations to sample amounts greater than 20 μg may result in error because of the fitting methods used. Among the three polymer–THF combinations tested, the above equations show that the ThFFF universal calibration parameters of the PMMA–THF combination are the least sensitive to sample mass changes while the highest selectivity (highest n value) is obtained. We indicated earlier[19–20] that the PMMA–THF combination is also the least sensitive to the cold wall temperature changes.

CONCLUSIONS

The change in R caused by a variation in sample mass from 1 to 20 μg can be as low as 3% for the smallest polymer (37 kg/mol PMMA) and as high as 35% for large polymers (1000 kg/mol PS).

The empirical equations relating n and ϕ_6 to m which were obtained in this study provide the ThFFF calibration curves needed to accurately determine polymer molecular weights using any ThFFF channel using the same T_c and ΔT at sample amounts from 0–20 μg. As indicated above, corrections for changes in T_c can be made empirically.[20]

The influence of the polymer on fluid viscosity within the sample zone appears to be the dominant factor affecting retention. This is because retention is seen to increase with increase of sample mass. We would expect retention to decrease with increase of sample mass if increased diffusion were the dominant factor. Finally, the present study suggests that it is very doubtful that there is some threshold sample mass below which retention is independent of sample mass.

Acknowledgment

This work was supported by the National Science Foundation Grant No. CHE-9322472.

References

[1] Giddings, J.C. (1993). *Science*, **260**, 1456.
[2] Giddings, J.C. (1994). *Anal. Chem.*, **66**, 2783.
[3] Gao, Y. and Chen, X. (1992). *J. Appl. Polym. Sci.*, **45**, 887.
[4] Sisson, R.M. and Giddings, J.C. (1994). *Anal. Chem.*, **66**, 4043.

[5] Nguyen, M.T. and Beckett, R. (1993). *Polym. Int.*, **30**, 337.
[6] Caldwell, K.D., Brimhall, S.L., Gao, Y. and Giddings, J.C. (1988). *J. Appl. Polym. Sci.*, **36**,703.
[7] Giddings, J.C., Yang, F.J.F. and Myers, M.N. (1974). *Anal. Chem.*, **46**, 1917.
[8] Brandrup, J. and Immergut, E.H. (1989). *Polymer Hand Book*; 3rd ed. (John Wiley & Sons, New York), p. 183.
[9] Gunderson, J.J., Caldwell, K.D. and Giddings, J.C. (1984). *Sep. Sci. Technol.*, **19**, 667.
[10] Streeter, D.J. and Boyer, R.F. (1954). *J. Polym. Sci.*, **14**, 5.
[11] Yu, T.L., Reihanian, H., Southwick, J.G. and Jamieson, A.M. (1981). *J. Macromol. Sci. Phys.*, **B18**, 777.
[12] Callaghan, P.T. and Pinder, D.N. (1980). *Macromolecules*, **13**, 1085.
[13] Tan, H., Moet, A., Hiltner, A. and Baer, E. (1983). *Macromolecules*, **16**, 28.
[14] Hoffman, J.D. and Zimm, B.H. (1955). *J. Polym. Sci.*, **XV**, 405.
[15] Whitmore, F.C. (1960). *J. Appl. Phys.*, **31**, 1858.
[16] Schimpf, M.E. and Giddings, J.C. (1989). *J. Polym. Sci. Part B: Polym. Phys.*, **27**, 1317.
[17] Schimpf, M.E. and Giddings, J.C. (1990). *J. Polym. Sci. Part B: Polym. Phys.*, **28**, 2673.
[18] Meyerhoff, V.G. and Rauch, B. (1969). *Makromol. Chem.*, **127**, 214.
[19] Myers, M.N., Cao, W.J., Chen, C.I., Kumar, V. and Giddings, J.C. (1997). *J. Liq. Chromatogr. Rel. Technol.*, **20**, 2757.
[20] Cao, W.J., Myers, M.N., Williams, P.S. and Giddings, J.C. (1997). *Anal. Chem.*, Submitted.
[21] Venema, E., de Leeuw, P., Kraak, J.C., Poppe, H. and Tijssen, R. (1997). *J. Chromatogr. A*, **765**, 135.
[22] van Asten, A.C., Kok, W.T., Tijssen, R. and Poppe, H. (1994). *J. Chromatogr. A*, **676**, 361.
[23] Mandema, W. and Zeldenrust, H. (1977). *Polymer*, **18**, 835.